Angewandte Chemie
Eine Zeitschrift der Gesellschaft Deutscher Chemiker

Supporting Information

© Wiley-VCH 2012

69451 Weinheim, Germany

A High Anisotropy Barrier in a Sulfur-Bridged Organodysprosium Single-Molecule Magnet**

Floriana Tuna, Charlene A. Smith, Michael Bodensteiner, Liviu Ungur, Liviu F. Chibotaru, Eric J. L. McInnes, Richard E. P. Winpenny, David Collison, and Richard A. Layfield**

anie_201202497_sm_miscellaneous_information.pdf

Section 1. Synthesis and X-ray crystallography: general considerations

Solvents were dried by refluxing under nitrogen over sodium-potassium alloy. Solids were manipulated using an MBraun LabMaster glovebox under an argon atmosphere, and solutions were transferred using a Schlenk line under nitrogen that had been passed through several columns of drying agents and a heated copper catalyst. Both *tris(*methylcyclopentadienyl)dysprosium and *tris(*methylcyclopentadienyl)gadolinium were synthesized according to literature procedures.[1] Single crystal X-ray diffraction data were collected either using an Oxford Diffaction Gemini R Ultra diffractometer (**1**) or an Oxford Instruments XCalibur2 diffractometer (**2**). Structures were solved and refined with SHELX.[2] For the refinement of the disordered phenyl and Cp parts of the structures, displacement parameter restraints were applied to the model. NMR spectra of lithium triphenylsilylthiolate were acquired using a Bruker Avance III spectrometer.

Synthesis of lithium triphenylsilylthiolate, Ph_3SiSLi. A stirred suspension of triphenylsilylthiol (Ph_3SiSH, 5.00 g, 17.1 mmol) in hexane (50 mL) was cooled to –78°C, and a solution of *n*-butyllithium in hexanes (1.6 M, 11.2 mL, 18.0 mmol, 5% excess) was added drop-wise over five minutes. The milky-white reaction mixture was warmed to room temperature and then treated with ultrasound for 15 minutes. Stirring the reaction overnight resulted in the formation of a colourless solid, which was collected on a porosity 3 frit, washed with hexane (3× 10 mL) and then dried *in vacuo*. Lithium triphenylsilylthiolate, Ph_3SiSLi, was obtained as a colourless solid (4.44 g, 87%). Elemental analysis calculated for $C_{18}H_{15}LiSiS$: C 72.45, H 5.07; found C 72.30, H 4.90. ^{1}H NMR (thf-d_8, 400.13 MHz, 298 K, δ/ppm): 7.698-7.722, multiplet, 6 ^{1}H, phenyl; 7.114-7.146, multiplet, 9 ^{1}H, phenyl. ^{7}Li NMR (thf-d_8, 155.51 MHz, 298 K): 0.567 ppm.

Synthesis of $[(C_5H_4Me)_2Gd(\mu\text{-}SSiPh_3)]_2\cdot$(toluene), 1·(toluene). A Schlenk tube was charged with $[(C_5H_4Me)_3Gd]$ (0.10 g, 0.25 mmol) and Ph_3SiSLi (0.076 g, 0.25 mmol) and cooled to –10°C. Toluene (20 mL) was added and the mixture warmed to room temperature and then stirred overnight, producing a light yellow solution with a gelatinous precipitate. The reaction mixture was filtered (Celite, porosity 3) and the frit then washed with toluene until the filtrate became colourless (5 mL). The solvent volume was reduced until copious amounts of a colourless precipitate had formed on the walls of the Schlenk tube, at which point the solution was gently heated until all the precipitate had re-dissolved. Storage of the light yellow solution at –30°C overnight produced colourless crystalline blocks, which X-ray crystallography subsequently revealed to be $[(C_5H_4Me)_2Gd(\mu\text{-}SSiPh_3)]_2\cdot$(toluene), **1**·(toluene). Placing **1**·(toluene) under vacuum for periods of about 30 minutes results in removal of the lattice toluene, giving **1** (0.097 g, 64% based on gadolinium). Elemental analysis calculated for $C_{60}H_{58}Si_2S_2Gd_2$: C 59.37, H 4.82; found C 59.03, H 4.77.

Synthesis of $[(C_5H_4Me)_2Dy(\mu\text{-}SSiPh_3)]_2\cdot$(toluene), 2·(toluene). The procedure used to synthesize **2·(toluene)** was identical to that used for the gadolinium analogue, with the following amounts: $[(C_5H_4Me)_3Dy]$ (0.10 g, 0.25 mmol), Ph_3SiSLi (0.076 g, 0.25 mmol) and toluene (20 mL). The bright yellow solution was stored at –30°C overnight, which produced yellow crystalline blocks, which X-ray crystallography subsequently revealed to be $[(C_5H_4Me)_2Dy(\mu\text{-}SSiPh_3)]_2\cdot$(toluene), **2**·(toluene). Placing **2**·(toluene) under vacuum for periods of about 30 minutes results in removal of the lattice toluene, giving **2** (0.120 g, 70% based on dysprosium). Elemental analysis calculated for $C_{60}H_{58}Si_2S_2Dy_2$: C 58.86, H 4.77; found C 58.71, H 4.69.

1. Wilkinson, G.; Birmingham, J. M. *J. Am. Chem. Soc*. **1954**, *76*, 6210.
2. Sheldrick, G. M. *Acta Cryst*. **2008**, *A64*, 112.

Table S1. Crystal data and structure refinement for **1**·(toluene)

Empirical formula	$C_{67}H_{66}Gd_2S_2Si_2$
Formula weight	1306.02
Temperature	123(1) K
Wavelength	1.54178 Å
Crystal system	Monoclinic
Space group	$P2_1/n$
Unit cell dimensions	a = 9.7437(2) Å
	b = 18.8921(6) Å β = 96.694(2)°
	c = 15.4871(5) Å
Volume	2831.41(14) Å^3
Z	2
Density (calculated)	1.532 Mg/m^3
Absorption coefficient	16.384 mm^{-1}
Crystal size	0.16 × 0.08 × 0.06 mm^3
Theta range for data collection	3.71 to 62.09°
Index ranges	-11<=h<=11, -21<=k<=20, -14<=l<=17
Reflections collected	11191
Independent reflections	4356 [R(int) = 0.0542]
Completeness to theta = 62.09°	97.8 %
Absorption correction	Semi-empirical from equivalents
Refinement method	Full-matrix least-squares on F^2
Data / restraints / parameters	4356 / 24 / 408
Goodness-of-fit on F^2	1.096
Final R indices [I>2σ(I)]	R_1 = 0.0469, wR_2 = 0.1222
R indices (all data)	R_1 = 0.0529, wR_2 = 0.1299
Largest diff. peak and hole	0.752 and -1.917 e.Å^{-3}

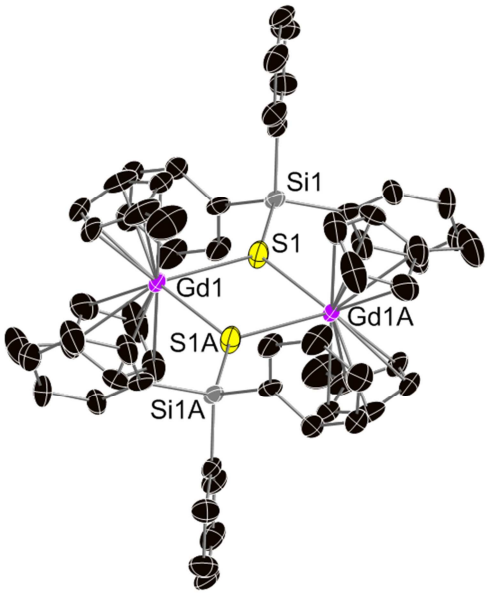

Figure S1. Thermal ellipsoid representation (50% probability) of the molecular structure of **1**.

Table S2. Crystal data and structure refinement for **2**·(toluene)

Empirical formula	$C_{67}H_{66}Dy_2S_2Si_2$
Formula weight	1316.52
Temperature	100(2) K
Wavelength	0.71073 Å
Crystal system	Monoclinic
Space group	$P2_1/n$
Unit cell dimensions	a = 9.7223(19) Å
	b = 18.864(4) Å β = 96.55(3)°
	c = 15.410(3) Å
Volume	2807.8(10) Å^3
Z	2
Density (calculated)	1.557 Mg/m^3
Absorption coefficient	2.799 mm^{-1}
Crystal size	0.70 × 0.10 × 0.10 mm^3
Theta range for data collection	1.71 to 28.83°.
Index ranges	-12<=h<=12, -24<=k<=24, -19<=l<=20
Reflections collected	24579
Independent reflections	6833 [R(int) = 0.0451]
Completeness to theta = 25.00°	100%
Absorption correction	Semi-empirical from equivalents
Refinement method	Full-matrix least-squares on F^2
Data / restraints / parameters	6833 / 36 / 407
Goodness-of-fit on F^2	1.127
Final R indices [I>2σ(I)]	R_1 = 0.0400, wR_2 = 0.0949
R indices (all data)	R_1 = 0.0559, wR_2 = 0.1183
Largest diff. peak and hole	1.327 and -1.125 e.Å^{-3}

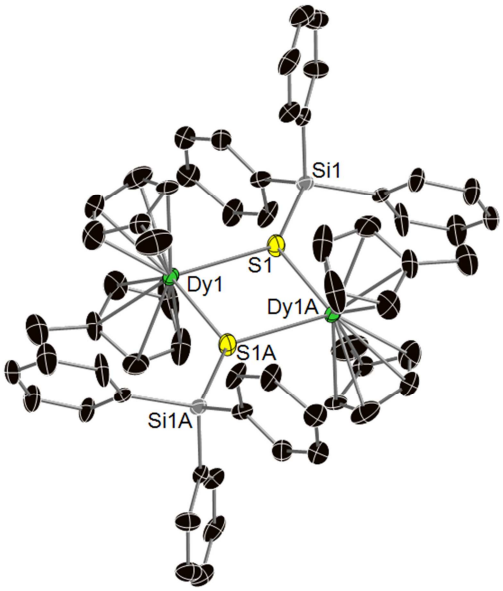

Figure S2. Thermal ellipsoid representation (50% probability) of the molecular structure of **2**.

Section 2. Magnetic susceptibility measurements on 1 and 2

The magnetic properties of polycrystalline samples of **1** and **2** were measured using a Quantum Design MPMS-7 SQUID magnetometer at temperatures in the range 1.8-300 K. In a glove box, the polycrystalline samples were transferred to Kel-F capsules, which were then sealed with an O-ring cap, and the capsules were then placed in plastic straws. One end of the straw was then sealed with a cap, and the other end was sealed with Blu-Tac. The straw was then sealed in a Schlenk tube and taken to the magnetometer. The straw was removed from the Schlenk tube and the Blu-Tac quickly replaced with the carbon fibre rod, and then the sample was quickly transferred to the purged sample space of the MPMS.

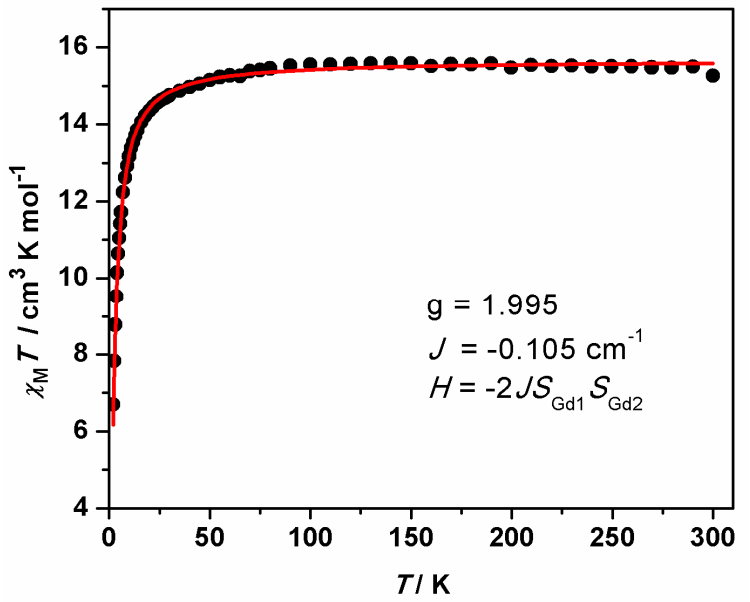

Figure S3. The product of molar magnetic susceptibility and temperature, $\chi_M T$, against temperature, T, for **1**. The red line is a theoretical fit of the experimental data using the spin Hamiltonian $H = -2J[S_{Gd1} \cdot S_{Gd1A}]$ and $g = 1.995$, which produced an exchange coupling constant of $J = -0.105$ cm^{-1}.

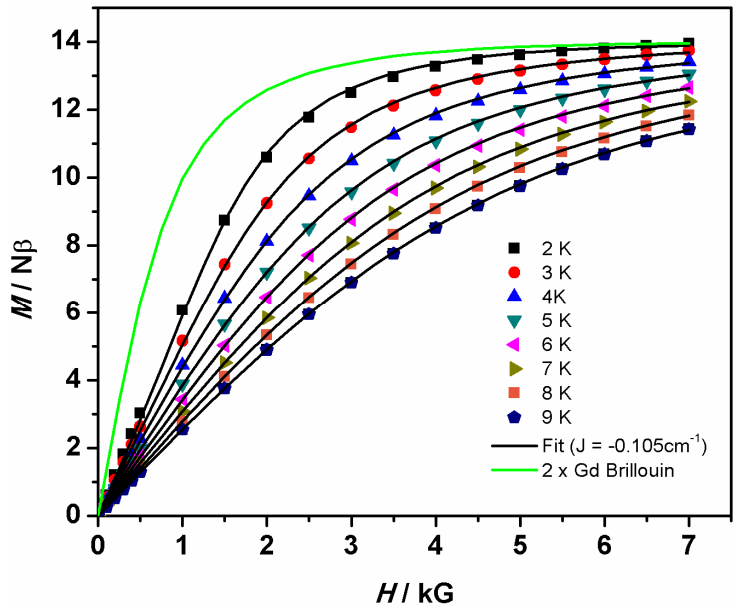

Figure S4. Plot of magnetization against field for **1** at various temperatures in the range 2-9 K. The solid lines are a theoretical fit of the experimental data using $J = -0.105$ cm^{-1}.

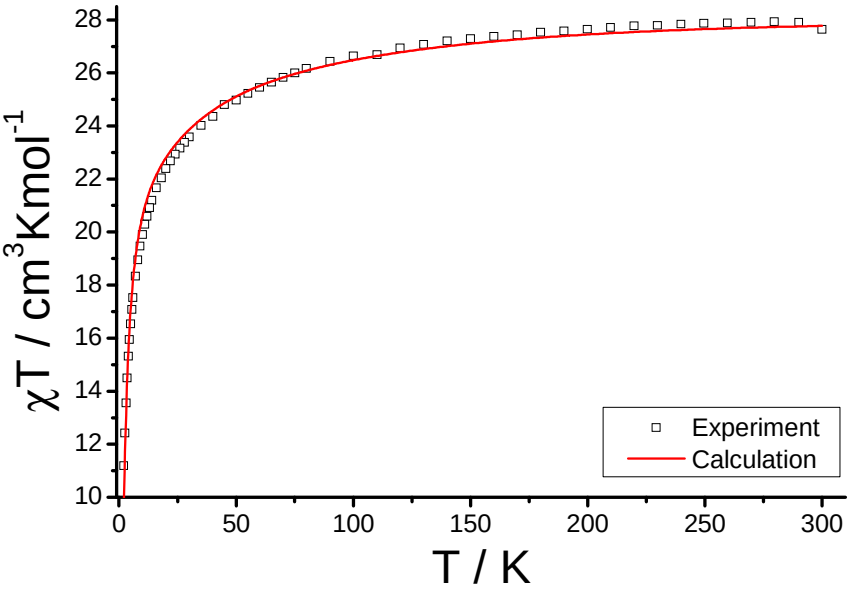

Figure S5. Product of molar magnetic susceptibility and temperature, $\chi_M T$, against temperature, T, for **2**. The red trace shows the calculated curve using the *ab initio* results in the computational model CB (see the details in Section 3 of the SI).

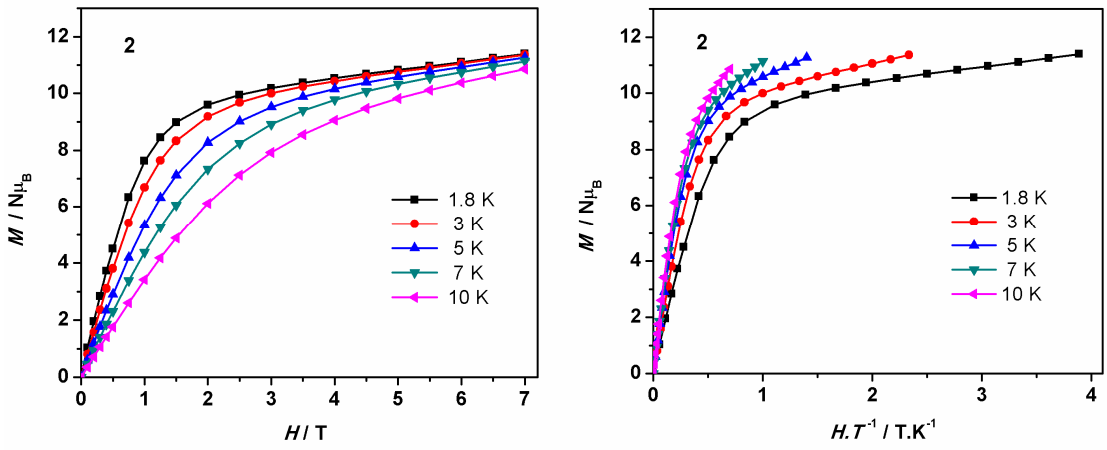

Figure S6. Left: M vs. H and; right, M vs. H/T for **2** at temperatures between 1.8 and 10 K.

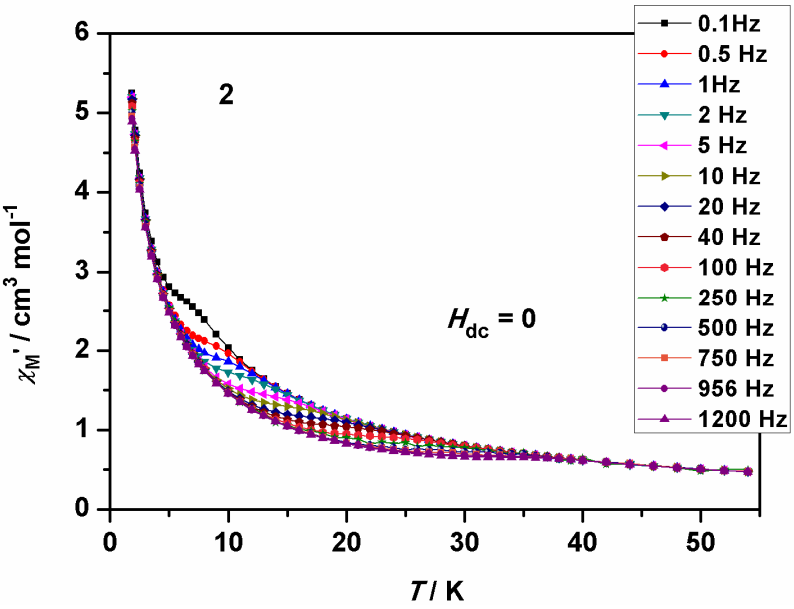

Figure S7. Temperature dependence of the in-phase ac susceptibility of **2** at zero-dc field and 1.55 Oe ac field, oscillating at the indicated frequencies.

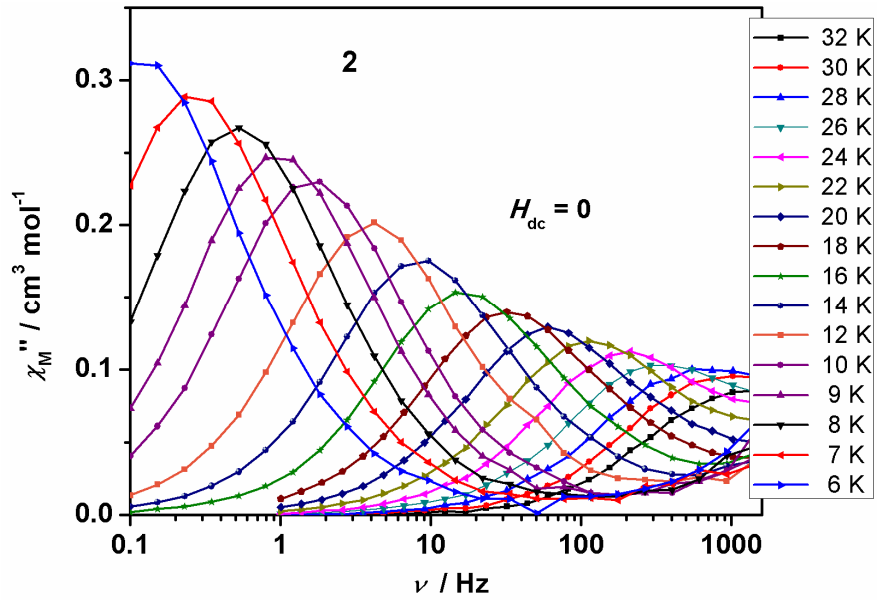

Figure S8. Frequency dependence in zero-dc-field of the out-of-phase (χ_M'') ac susceptibility of **2** at temperatures between 6 and 32 K.

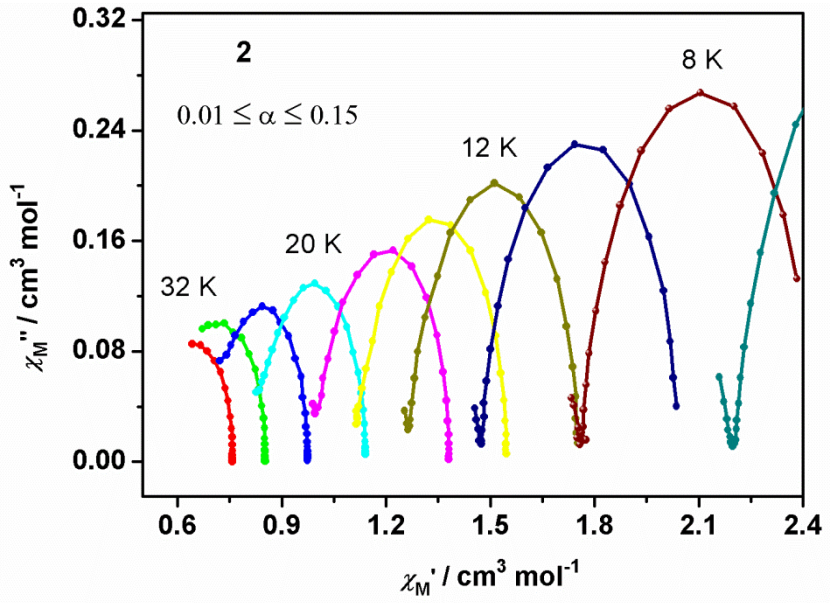

Figure S9. Cole-Cole diagram for **2** at temperatures in the range 28 and 18 K.

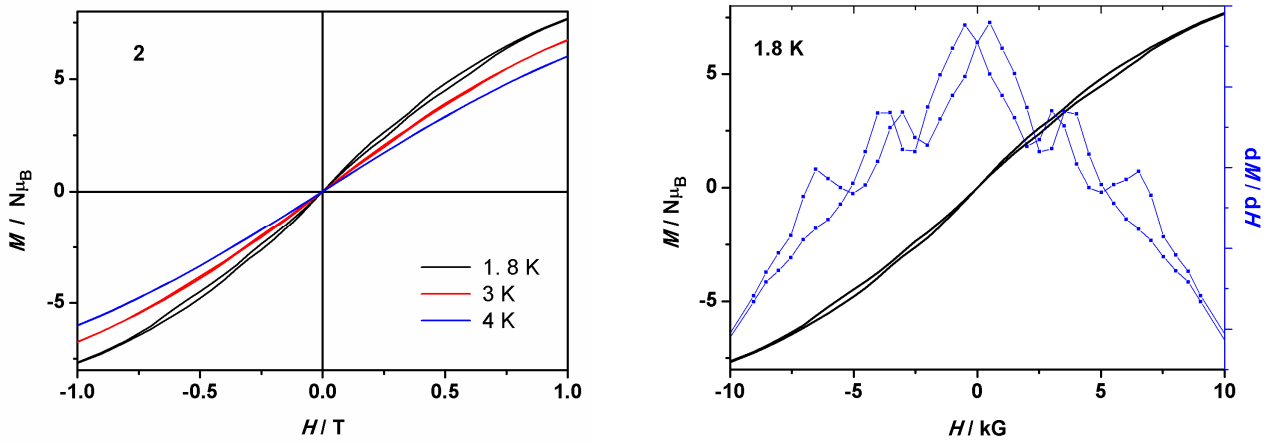

Figure S10. Left: magnetization versus field plots for **2** at T = 1.8, 3 and 4 K. Right: magnetization versus field plots for **2** at T = 1.8 K and plot of dM/dH *vs.* H.

Section 3. *Ab initio* Calculations of electronic and magnetic properties

Computational details: All calculations were done with MOLCAS 7.6 and are of the CASSCF/RASSI/SINGLE_ANISO type.

$[(C_5H_4Me)_2Ln(\mu\text{-}SSiPh_3)]_2$ (2)

We have employed three structural approximations: **A**, a reduced fragment of the molecule; **B**, a larger fragment, and; C, the entire molecule. Each structural approximation was calculated using two basis set approximations: **A** small, and **B** large. This results in six computational approximations for **2**, i.e. **AA**, **AB**, **BA**, **BB, CA** and **CB**.

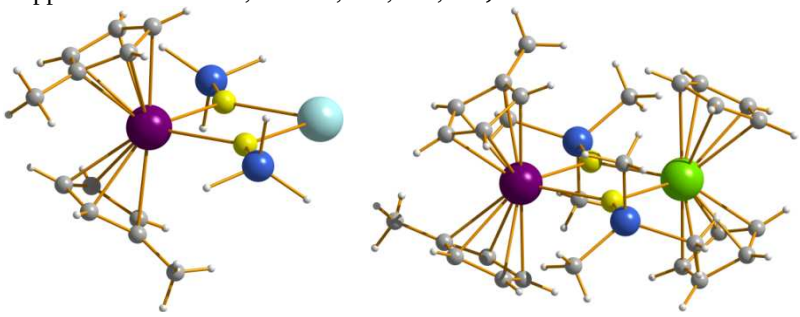

Figure S11. Structure of the calculated fragment **A** (left) and **B** (right) of **2**. Color scheme: Dy - violet, Lu – green, La – light turquoise, Si – blue, S – yellow, C – grey, H – white.

$[Cp_2Dy(\mu\text{-}Cl)]_2$ (3a)

We have employed two structural approximations: **A**, a reduced fragment of the molecule, and; **B**, the entire molecule. Each structural approximation was calculated using two basis set approximations: **A** small, and **B** large. This results in four computational approximations for **3a**, **AA**, **AB**, **BA**, and **BB**.

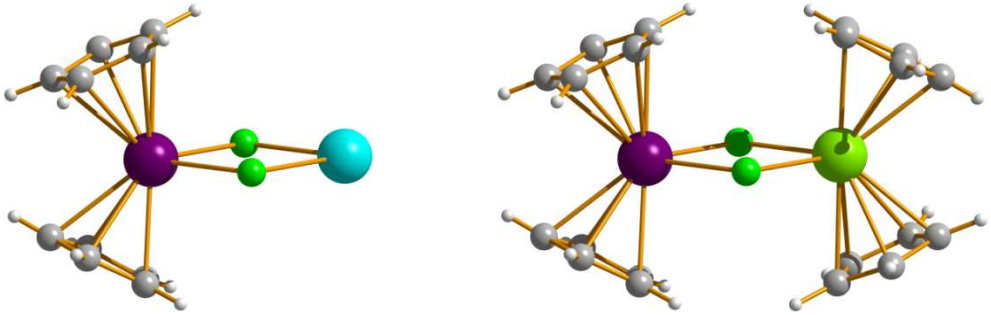

Figure S12. Structure of the calculated fragment **A** (left) and **B** (right) of the complex **3 –dimer**. Color scheme: Dy - violet, Lu – light green, La – green, Cl – yellow, O – red, C – grey, H – white.

$[Cp_2Dy(\mu\text{-}Cl)]_\infty$ (3b)

We have employed two structural approximations: **A**, a reduced fragment of the molecule, and; **B**, the entire molecule. Each structural approximation was calculated using two basis set approximations: **A** small, and **B** large. This results in four computational approximations for **3a**, **AA**, **AB**, **BA**, and **BB**.

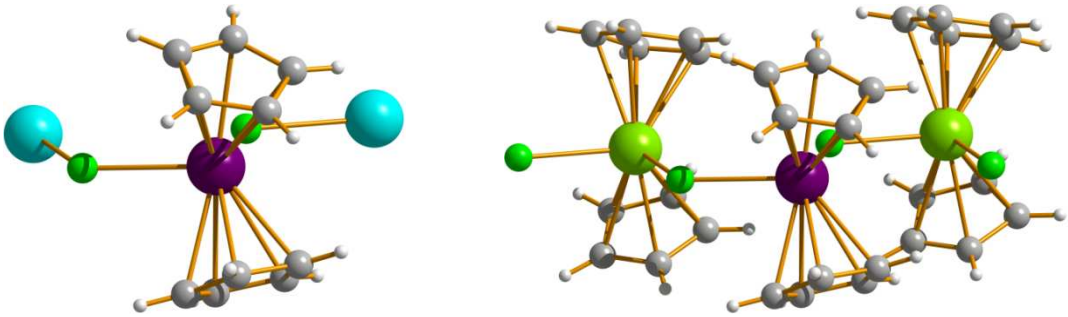

Figure S13. Structure of the calculated fragment **A** (left) and **B** (right) of the complex **3 – polymer**. Color scheme: Dy - violet, La – green, Lu – light green, Cl – yellow, O – red, C – grey, H – white.

$[Cp_2Dy(thf)(\mu\text{-}Cl)]_2$ (4)

We have employed two structural approximations: **A**, a reduced fragment of the molecule, and; **B**, the entire molecule. Each structural approximation was calculated using two basis set approximations: **A** small, and **B** large. This results in four computational approximations for **3a**, **AA**, **AB**, **BA**, and **BB**.

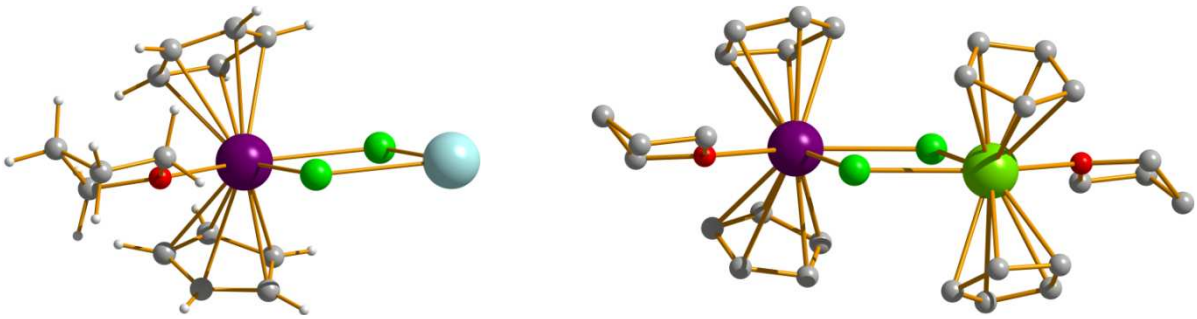

Figure S14. Structure of the fragment **A** (left) and B (right) of the complex **4**. Color scheme: Dy - violet, La – cyan, Lu – light green, Cl – green, O – red, C – grey, H – white.

$[Cp_2Dy(\mu\text{-Bta})]_2$ (5)

We have employed two structural approximations: **A**, a reduced fragment of the molecule, and; **B**, the entire molecule. Each structural approximation was calculated using two basis set approximations: **A** small, and **B** large. This results in four computational approximations for **3a**, **AA**, **AB**, **BA**, and **BB**.

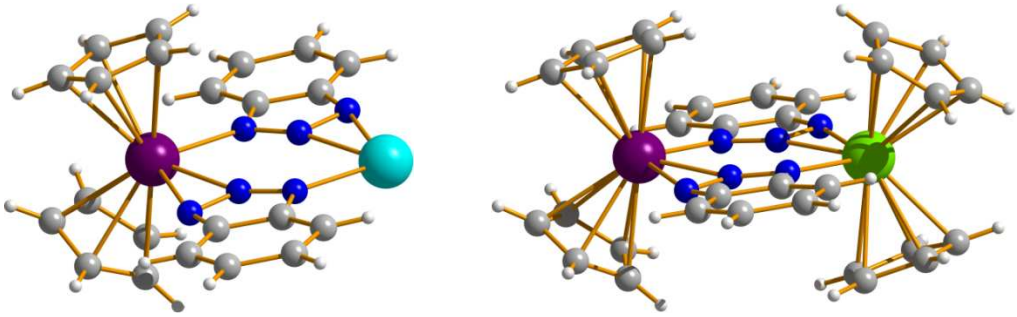

Figure S15. Structure of the calculated fragment **A** (left) and **B** (right) of the complex **5**. Color scheme: Dy - violet, La- cyan, Lu – green, N – blue, C – grey, H – white.

Table S3. Contractions of the employed basis sets in computational approximations **A** and **B**.

Basis A	Basis B
Dy.ANO-RCC...7s6p4d3f1g.	Dy.ANO-RCC...8s7p5d4f2g1h.
La.ECP.deGraaf.0s.0s.0e-La(LaMnO3).	La.ECP.deGraaf.0s.0s.0e-La(LaMnO3).
Lu.ANO-RCC...7s6p4d3f1g.	Lu.ANO-RCC...7s6p4d3f1g.
Si.ANO-RCC...4s3p.	Si.ANO-RCC...5s4p2d.
S.ANO-RCC...4s3p1d.	S.ANO-RCC...5s4p2d1f.
Cl.ANO-RCC...4s3p1d.	Cl.ANO-RCC...5s4p2d1f.
O.ANO-RCC...3s2p1d.	O.ANO-RCC...4s3p2d1f. (close)
C.ANO-RCC...3s2p.	O.ANO-RCC...4s3p2d. (distant)
H.ANO-RCC...2s.	C.ANO-RCC...4s3p1d. (close)
	C.ANO-RCC...3s2p. (distant)
	H.ANO-RCC...2s1p.

Electronic and magnetic properties of $[(C_5H_4Me)_2Dy(\mu\text{-}SSiPh_3)]_2$ (2)

Table S4. Energies of the lowest Kramers doublets (cm^{-1}) in **2**.

Kramers doublets (cm^{-1})					
AA	AB	BA	BB	CA	CB
0.000	0.000	0.000	0.000	0.000	0.000
158.894	187.514	83.079	106.676	88.201	113.151
333.452	383.642	240.288	279.464	241.151	283.888
448.781	516.897	276.716	350.322	292.568	367.884
533.825	606.289	310.780	370.651	319.373	385.991
558.447	618.388	338.173	409.524	352.575	426.208
581.103	660.793	368.637	451.587	373.706	456.957
714.687	828.920	527.048	629.611	515.884	624.035
3613.458	3627.429	3588.728	3596.413	3587.652	3596.823
3788.221	3816.493	3705.215	3733.246	3710.833	3739.744
3888.975	3930.665	3740.002	3782.724	3750.951	3795.463
3973.137	4030.448	3788.946	3845.844	3799.613	3859.633
4059.552	4126.940	3859.017	3923.702	3870.000	3938.205
4116.181	4188.245	3913.162	3988.652	3917.349	3996.091
4153.402	4253.084	3969.571	4062.097	3961.650	4059.212
6197.038	6220.773	6138.681	6157.516	6139.480	6160.070
6342.943	6372.436	6236.967	6269.878	6244.952	6278.623
6424.048	6466.366	6265.800	6309.266	6276.979	6322.479
6517.252	6574.768	6335.952	6390.286	6343.658	6402.107
6603.579	6676.340	6420.697	6487.363	6424.396	6495.737
6645.207	6728.268	6453.525	6538.178	6451.157	6538.895
8201.238	8231.971	8117.161	8143.859	8119.140	8147.932
8320.770	8353.059	8191.792	8230.027	8200.504	8240.195
8405.617	8450.215	8231.929	8277.158	8243.751	8291.414
8509.489	8579.165	8350.262	8409.053	8349.544	8414.498
8582.294	8653.777	8393.263	8467.328	8395.993	8471.681
9752.228	9783.879	9660.971	9686.961	9664.026	9692.289
9868.246	9900.570	9722.806	9761.482	9732.868	9773.636
9981.179	10043.370	9790.402	9850.645	9798.008	9861.683
10118.492	10187.185	9952.612	10018.883	9952.194	10021.689
…	…	…	…	…	…

Table S5. Energies (cm^{-1}) and *g* tensors of the lowest Kramers doublets (KD) in **2**.

KD		AA		AB		BA		BB		CA		CB	
		E	*g*	E	*g*	E	*g*	E	*g*	E	*g*	E	*g*
1	g_X	0.000	0.0000	0.000	0.0001	0.000	0.0029	0.000	0.0011	0.000	0.0031	0.000	0.0012
	g_Y		0.0005		0.0003		0.0056		0.0021		0.0050		0.0019
	g_Z		19.6856		19.7150		19.0827		19.2880		19.1740		19.3611
2	g_X	158.894	0.0025	187.514	0.0020	83.079	0.0022	106.676	0.0018	88.201	0.0037	113.151	0.0029
	g_Y		0.0032		0.0023		0.0082		0.0039		0.0094		0.0049
	g_Z		17.1491		17.1095		17.0666		17.0284		17.0928		17.0545
3	g_X	333.452	0.1432	383.642	0.0726	240.288	0.2870	279.464	0.0795	241.151	0.1878	283.888	0.0726
	g_Y		0.1844		0.0843		0.3526		0.0992		0.2597		0.0858
	g_Z		14.6263		14.6204		15.1700		15.0123		15.1391		14.9721
4	g_X	448.781	0.5212	516.897	0.5406	276.716	1.3632	350.322	0.6476	292.568	3.3772	367.884	8.7803
	g_Y		0.6543		0.6295		1.7863		1.7005		4.3149		6.8391
	g_Z		11.4535		11.7317		16.4165		16.7454		12.5142		1.8084
5	g_X	533.825	2.1236	606.289	0.1044	310.780	0.8760	370.651	1.0223	319.373	7.8279	385.991	0.2759
	g_Y		3.7318		1.1238		4.1547		3.7009		5.3026		4.6117
	g_Z		6.8870		11.8660		10.0511		10.4453		2.4932		11.8435
6	g_X	558.447	1.5240	618.388	2.1563	338.173	1.1825	409.524	3.8555	352.575	0.8819	426.208	2.3401
	g_Y		2.5609		2.7647		3.3415		4.8097		3.1923		5.1644
	g_Z		17.6417		11.5628		13.6435		11.7483		13.7867		11.0989
7	g_X	581.103	2.9191	660.793	11.6524	368.637	1.9407	451.587	0.9977	373.706	1.5548	456.957	1.0027
	g_Y		4.6242		7.5952		5.7089		2.8156		6.2898		3.8534
	g_Z		13.6088		2.6082		13.0187		15.1869		12.2011		13.8268
8	g_X	714.687	0.0376	828.920	0.0220	527.048	0.0971	629.611	0.0687	515.884	0.1325	624.035	0.0836
	g_Y		0.1471		0.0715		0.1322		0.0948		0.1932		0.1247
	g_Z		19.5754		19.6455		19.7197		19.7552		19.6713		19.7289

Table S6. Angles [°] between the main magnetic axes of the lowest Kramers doublet in **2**, obtained in different computational approximations.

	AA	AB	BA	BB	CA	CB
AA	0.000	0.182	3.007	2.291	2.234	1.657
AB	0.182	0.000	3.034	2.311	2.269	1.681
BA	3.007	3.034	0.000	0.727	0.779	1.353
BB	2.291	2.311	0.727	0.000	0.200	0.635
CA	2.234	2.269	0.779	0.200	0.000	0.594
CB	1.657	1.681	1.353	0.635	0.594	0.000

The main anisotropy axis of the ground state is almost perpendicular to the Dy_2S_2 plane (see Table S7).

Table S7. Angles [°] between the main magnetic axes of the lowest Kramers doublet in **2**, obtained in different computational approximations and the Dy_2S_2 plane (degrees).

	AA	AB	BA	BB	CA	CB
angle	86.232	86.308	83.317	84.043	84.059	84.653

The orientation of the main anisotropy axes in the ground Kramers doublet of **2**, with an illustration of the antiferromagnetic coupling of the local Dy magnetic moments, is shown in the main article (Figure 4).

Table S8. Exchange interactions between Dy ions in **2**.
Lines parameters (cm^{-1}):

	AA	AB	BA	BB	CA	CB
J_{exch}	-0.09234	-0.09177	-0.08569	-0.08704	-0.08649	-0.08779
$J_{dipolar}$	-0.09037	-0.09038	-0.08764	-0.08842	-0.08846	-0.08902
$J_{total}=J_{exch}+J_{dipolar}$	-0.18271	-0.18215	-0.17333	-0.17546	-0.17495	-0.17681

Ising parameters (cm^{-1}):

	AA	AB	BA	BB	CA	CB
J_{exch}	-2.30850	-2.29425	-2.14225	-2.17600	-2.16225	-2.19475
$J_{dipolar}$	-2.25925	-2.25950	-2.19100	-2.21050	-2.21150	-2.22550
$J_{total}=J_{exch}+J_{dipolar}$	-4.56775	-4.55375	-4.33325	-4.38650	-4.37375	-4.42025

Table S9. Energies and corresponding tunnelling gaps of the lowest five exchange doublet states of **2**.
Part 1:

AA		AB		BA	
energy	Δ_t	energy	Δ_t	energy	Δ_t
0.000000000 0.000000000	0.00000E+00	0.000000000 0.000000000	0.00000E+00	0.000000000 0.000000033	3.30000E-08
2.145312760 2.145313134	3.74000E-07	2.145050520 2.145051601	1.08100E-06	1.918489585 1.918489858	2.73000E-07
158.936768811 158.936768837	2.60000E-08	187.558754213 187.558754220	7.00001E-09	83.063830893 83.063831680	7.87000E-07
159.134766976 159.134766998	2.20000E-08	187.761670581 187.761670586	5.00000E-09	83.279366718 83.279367275	5.57000E-07
160.886202287 160.886203526	1.23900E-06	189.505048433 189.505048693	2.60000E-07	84.835466373 84.835467671	1.29800E-06

Part 2:

BB		CA		CB	
energy	Δ_t	energy	Δ_t	energy	Δ_t
0.000000000 0.000000005	5.00000E-09	0.000000000 0.000000007	7.00000E-09	0.000000000 0.000000001	1.00000E-09
1.982829107 1.982829965	8.58000E-07	1.954021209 1.954024704	3.49500E-06	2.012402293 2.012402371	7.80000E-08
106.680340911 106.680341051	1.40000E-07	88.196463276 88.196463890	6.14000E-07	113.163773254 113.163773370	1.16000E-07
106.892646092 106.892646201	1.09000E-07	88.406351627 88.406351987	3.60000E-07	113.372241800 113.372241876	7.60000E-08
108.493021565 108.493022023	4.58000E-07	89.992314081 89.992315957	1.87600E-06	114.998454316 114.998454636	3.20000E-07

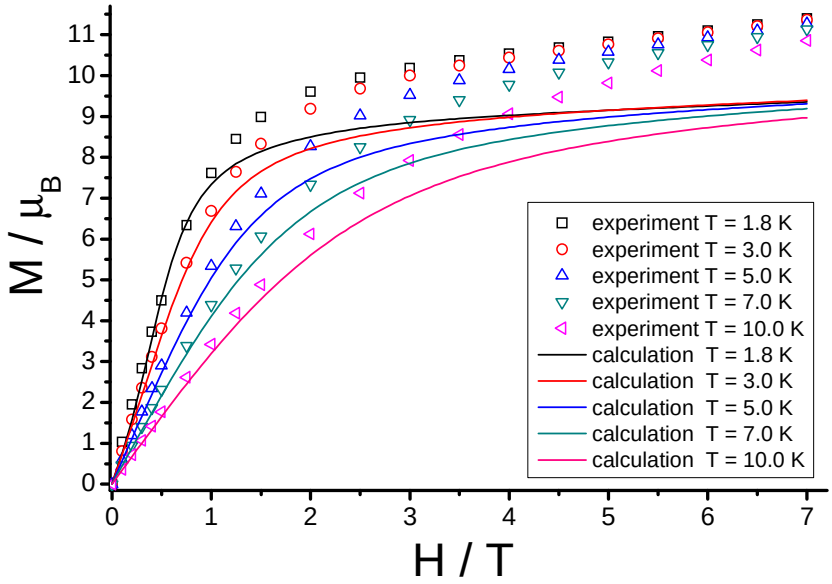

Figure S16. Measured and calculated molar magnetization of **2** at low temperatures (computational approximation CB).

Electronic and magnetic properties of $[Cp_2Dy(\mu\text{-}Cl)]_2$ (3a)

Table S10. Energies of the lowest Kramers doublets (cm^{-1}) on individual Dy ions.

Kramers doublets (cm^{-1})			
AA	AB	BA	BB
0.000	0.000	0.000	0.000
247.390	237.785	150.706	144.200
446.454	433.014	322.790	313.188
582.822	563.195	411.535	383.364
688.038	658.574	416.315	400.821
755.084	694.332	467.201	444.185
766.313	723.748	509.009	487.838
885.626	871.246	694.458	672.128
3661.795	3654.771	3619.668	3614.754
3856.114	3840.145	3762.374	3750.584
4011.291	3982.988	3832.255	3813.567
4130.583	4096.050	3906.541	3884.064
4227.292	4191.236	3984.472	3958.824
4289.538	4246.646	4049.832	4026.161
4319.032	4294.918	4125.584	4102.739
6272.790	6259.474	6194.594	6185.539
6420.768	6398.579	6303.352	6287.192
6551.821	6519.063	6360.696	6339.190
6677.226	6640.742	6452.884	6428.122
6765.720	6734.115	6549.839	6524.657
6811.856	6775.424	6602.286	6578.302
8294.988	8275.995	8188.961	8175.927
8411.363	8383.540	8268.498	8249.142
8549.181	8511.796	8337.402	8312.743
8667.740	8639.015	8472.310	8447.939
8739.831	8701.031	8529.291	8503.884
9850.461	9827.498	9731.794	9716.479
9971.381	9939.228	9807.262	9785.344
10151.807	10116.964	9926.471	9899.840
…	…	…	…

Table S11. Energies (cm^{-1}) and *g* tensors of the lowest Kramers doublets (KD) on individual Dy ions.

KD		AA		AB		BA		BB	
		E (cm^{-1})	*g*	E (cm^{-1})	*g*	E (cm^{-1})	*g*	E (cm^{-1})	*g*
1	g_X	0.000	0.0007	0.000	0.0005	0.000	0.0001	0.000	0.0004
	g_Y		0.0009		0.0008		0.0007		0.0009
	g_Z		19.7544		19.7260		19.4443		19.4090
2	g_X	247.390	0.0051	237.785	0.0006	150.706	0.0063	144.200	0.0066
	g_Y		0.0055		0.0010		0.0074		0.0078
	g_Z		17.0949		17.0777		16.9821		16.9597
3	g_X	446.454	0.1533	433.014	0.1477	322.790	0.0448	313.188	0.0050
	g_Y		0.1856		0.1750		0.0483		0.0097
	g_Z		14.4280		14.4867		14.7878		14.8008
4	g_X	582.822	0.2492	563.195	0.0502	411.535	0.0105	383.364	0.0372
	g_Y		0.5072		0.2636		1.5151		0.3037
	g_Z		11.5010		11.6394		15.5494		19.2969
5	g_X	688.038	3.7498	658.574	3.3567	416.315	1.1175	400.821	1.1703
	g_Y		4.6373		3.6838		2.0917		1.4729
	g_Z		8.1679		8.6381		9.9559		11.6236
6	g_X	755.084	0.9324	694.332	1.3817	467.201	5.2542	444.185	5.3295
	g_Y		3.1856		3.6405		5.9350		5.6150
	g_Z		12.6032		15.8790		9.2976		10.2589
7	g_X	766.313	10.1472	723.748	10.5685	509.009	0.7956	487.838	0.4729
	g_Y		7.8019		8.6765		1.5741		1.4056
	g_Z		1.2881		1.9286		15.4520		15.8294
8	g_X	885.626	0.1177	871.246	0.0451	694.458	0.0443	672.128	0.0443
	g_Y		0.1972		0.0597		0.0741		0.0677
	g_Z		19.3054		19.4715		19.7135		19.7336

Table S12. Angles between the main magnetic axes of the lowest Kramers doublet obtained in different computational approximations (degrees).

	AA	AB	BA	BB
AA	0.000	0.228	1.288	1.834
AB	0.228	0.000	1.082	1.622
BA	1.288	1.082	0.000	0.553
BB	1.834	1.622	0.553	0.000

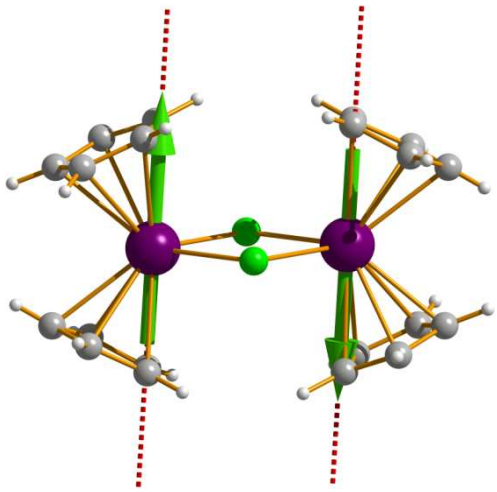

Figure S17. Orientation of the main anisotropy axes of the ground Kramers doublet of **3a**. Green arrows show the antiferromagnetic coupling of the local magnetic moments of the Dy ions in the ground state. The main anisotropy axis of the ground state is almost perpendicular to the Dy_2Cl_2 plane (see Table S13).

Table S13. Angles between the main magnetic axes of the lowest Kramers doublet, obtained in different computational approximations, and the Dy_2Cl_2 plane in **3a** [°].

	AA	AB	BA	BB
angle	87.424	87.251	86.185	85.672

Table S14. Exchange interactions between Dy ions in **3a**.

Lines parameters (cm^{-1}):

	AA	AB	BA	BB
J_{exch}	0.00000	0.00000	0.00000	0.00000
$J_{dipolar}$	-0.10526	-0.10506	-0.10267	-0.10268
$J_{total}=J_{exch}+J_{dipolar}$	-0.10526	-0.10506	-0.10267	-0.10268

Ising parameters (cm^{-1}):

	AA	AB	BA	BB
J_{exch}	0.00000	0.00000	0.00000	0.00000
$J_{dipolar}$	-2.63148	-2.62642	-2.56664	-2.56705
$J_{total}=J_{exch}+J_{dipolar}$	-2.63148	-2.62642	-2.56664	-2.56705

Only the intra-molecular dipolar interaction was considered.

Table S15. Energies and corresponding tunneling gaps of the lowest five exchange doublet states of **3a**.

AA		AB		BA		BB	
energy	Δ_t	energy	Δ_t	energy	Δ_t	energy	Δ_t
0.000000000 0.000000004	4.000E-09	0.000000000 0.000000004	4.000E-09	0.000000000 0.000000001	1.000E-09	0.000000000 0.000000001	1.000E-09
1.303359246 1.303360794	1.548E-06	1.298352720 1.298355544	2.824E-06	1.254173462 1.254177340	3.878E-06	1.244744735 1.244745246	5.110E-07
247.323142486 247.323142503	1.700E-08	237.713043881 237.713043907	2.600E-08	150.588507817 150.588507823	6.000E-09	144.075711941 144.075711942	1.000E-09
247.632211773 247.632211832	5.900E-08	238.030929182 238.030929214	3.200E-08	150.975157236 150.975157241	5.000E-09	144.470099170 144.470099178	8.000E-09
248.516176394 248.516178101	1.707E-06	238.899440511 238.899441083	5.720E-07	151.731882858 151.731884798	1.940E-06	145.214010194 145.214010454	2.600E-07

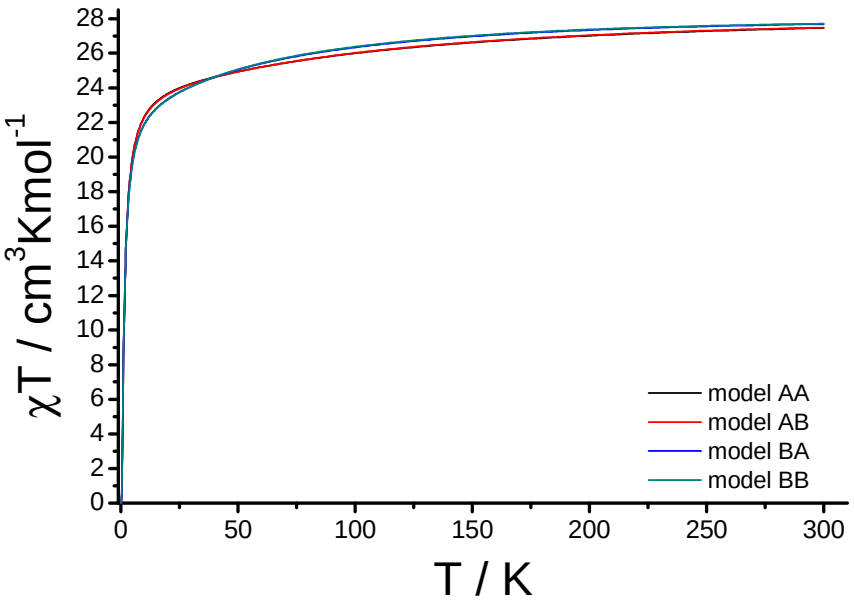

Figure S18. Calculated magnetic susceptibility of **3a**.

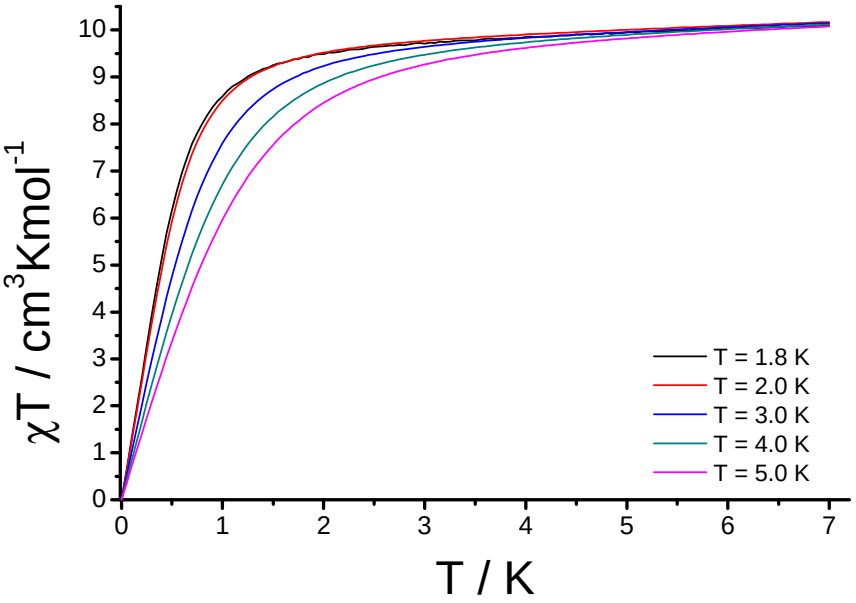

Figure S19. Calculated molar magnetization of **3a** at low temperatures (computational approximation BB).

Local electronic and magnetic properties of the chain $[Cp_2Dy(\mu\text{-}Cl)]_\infty$ (3b)

Table S16. Energies of the lowest Kramers doublets (cm^{-1}) on individual Dy ions in **3b**.

Kramers doublets (cm^{-1})			
AA	AB	BA	BB
0.000	0.000	0.000	0.000
280.148	272.508	136.272	134.432
516.890	500.919	300.671	296.615
680.076	656.399	365.031	356.800
778.127	748.084	399.656	392.299
846.915	810.952	444.274	434.601
939.038	897.205	467.611	457.868
1104.385	1061.111	599.178	588.890
3684.981	3676.574	3608.951	3605.449
3909.012	3891.514	3754.879	3748.329
4079.368	4054.963	3816.749	3808.024
4216.142	4186.377	3876.317	3866.286
4326.724	4292.373	3949.911	3938.218
4419.583	4379.792	3997.588	3985.289
4525.795	4480.535	4050.320	4038.416
6315.378	6300.084	6176.170	6170.279
6480.158	6457.496	6292.245	6283.151
6622.987	6594.787	6340.438	6329.671
6766.685	6733.459	6418.236	6405.978
6882.004	6844.657	6496.138	6482.992
6994.478	6948.279	6543.481	6529.916
8353.001	8331.546	8163.790	8155.597
8476.255	8449.631	8251.670	8240.784
8621.227	8589.573	8312.525	8299.949
8778.462	8742.755	8417.228	8403.856
8900.919	8855.144	8482.559	8467.672
9916.048	9890.803	9710.743	9701.030
10028.449	10000.240	9783.639	9771.676
10250.467	10214.894	9874.699	9861.103

Table S17. Energies (cm^{-1}) and *g* tensors of the lowest Kramers doublets (KD) on individual Dy ions in **3b**.

KD		AA		AB		BA		BB	
		E (cm^{-1})	*g*	E (cm^{-1})	*g*	E (cm^{-1})	*g*	E (cm^{-1})	*g*
1	g_X	0.000	0.0001	0.000	0.0001	0.000	0.0008	0.000	0.0009
	g_Y		0.0002		0.0002		0.0014		0.0015
	g_Z		19.7173		19.7088		19.3645		19.3590
2	g_X	280.148	0.0036	272.508	0.0031	136.272	0.0033	134.432	0.0032
	g_Y		0.0041		0.0035		0.0049		0.0049
	g_Z		16.9992		16.9988		17.0542		17.0444
3	g_X	516.890	0.0605	500.919	0.0516	300.671	0.2764	296.615	0.3412
	g_Y		0.0669		0.0570		0.4015		0.5087
	g_Z		14.2952		14.3148		14.7838		14.7502
4	g_X	680.076	1.0389	656.399	1.0290	365.031	3.6916	356.800	3.8036
	g_Y		1.4377		1.4235		5.6879		5.0426
	g_Z		11.0262		11.0598		10.6077		11.4057
5	g_X	778.127	4.9222	748.084	4.8129	399.656	2.0448	392.299	1.4211
	g_Y		5.3107		5.2718		3.6749		4.1913
	g_Z		9.2985		9.6030		9.4417		9.2551
6	g_X	846.915	0.0886	810.952	0.2568	444.274	2.0382	434.601	1.9024
	g_Y		1.1807		1.0256		3.9921		3.5564
	g_Z		13.1216		13.0862		14.1107		14.6637
7	g_X	939.038	0.5998	897.205	0.6578	467.611	0.3098	457.868	0.3156
	g_Y		0.9532		1.0781		2.1808		2.2447
	g_Z		16.8039		16.6697		14.8152		14.8224
8	g_X	1104.385	0.0176	1061.111	0.0147	599.178	0.1481	588.890	0.1435
	g_Y		0.0243		0.0218		0.2555		0.2358
	g_Z		19.4433		19.4516		19.5304		19.5528

Table S18. Angles between the main magnetic axes of the lowest Kramers doublet in **3b**, obtained in different computational approximations [°]

	AA	AB	BA	BB
AA	0.000	0.079	2.306	2.274
AB	0.079	0.000	2.368	2.336
BA	2.306	2.368	0.000	0.034
BB	2.274	2.336	0.034	0.000

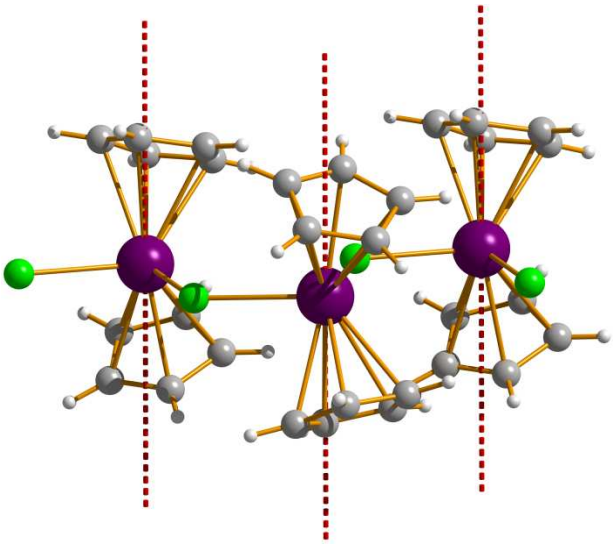

Figure S20. Orientation of the main anisotropy axes of the ground Kramers doublet of **3b**. The main anisotropy axis of the ground state is almost perpendicular to the Dy_2Cl_2 plane (see Table S19).

Table S19. Angles between the main magnetic axes of the lowest Kramers doublet, obtained in different computational approximations, and the Dy_2Cl_2 plane in **3b** [°].

	AA	AB	BA	BB
angle	86.730	86.809	84.737	84.763

Electronic and magnetic properties of $[Cp_2Dy(thf)(\mu\text{-}Cl)]_2$ (4)

Table S20. Energies of the lowest Kramers doublets (cm^{-1}) on individual Dy ions in **4**.

Kramers doublets (cm^{-1})			
AA	AB	BA	BB
0.000	0.000	0.000	0.000
161.847	159.094	97.646	95.851
290.283	286.670	199.378	192.583
359.280	352.868	217.607	211.385
431.146	424.226	239.960	235.811
480.015	464.923	293.116	285.788
540.820	511.156	316.491	308.481
593.619	561.349	347.899	338.596
3615.995	3612.236	3599.036	3597.358
3761.994	3753.888	3687.245	3680.693
3854.310	3842.610	3720.764	3711.712
3908.744	3896.987	3751.453	3741.328
3949.800	3934.302	3788.534	3781.157
4004.998	3984.065	3810.012	3798.763
4095.644	4061.705	3838.705	3827.819
6188.011	6180.611	6131.645	6127.080
6305.804	6294.212	6210.007	6201.593
6385.681	6370.802	6252.257	6241.480
6441.815	6426.223	6280.209	6268.865
6484.061	6465.088	6319.894	6310.546
6589.880	6557.781	6349.688	6336.395
8176.579	8166.047	8093.109	8086.191
8276.750	8261.820	8150.218	8139.828
8365.182	8347.640	8219.005	8206.755
8402.026	8384.866	8263.264	8253.370
8522.563	8492.202	8304.645	8290.177
9724.811	9712.908	9644.164	9636.018
9824.725	9807.215	9681.412	9669.924
9892.995	9875.198	9727.124	9715.189
10059.817	10030.842	9872.958	9858.250
…	…	…	…

Table S21. Energies (cm^{-1}) and *g* tensors of the lowest Kramers doublets (KD) on individual Dy ions in **4**.

KD		AA		AB		BA		BB	
		E (cm^{-1})	*g*	E (cm^{-1})	*g*	E (cm^{-1})	*g*	E (cm^{-1})	*g*
1	g_X	0.000	0.0015	0.000	0.0017	0.000	0.0183	0.000	0.0224
	g_Y		0.0020		0.0021		0.0377		0.0479
	g_Z		19.6482		19.6324		18.9781		18.9208
2	g_X	161.847	0.0681	159.094	0.0583	97.646	0.1143	95.851	0.1665
	g_Y		0.1111		0.0939		0.1475		0.1983
	g_Z		17.0341		17.0445		16.8076		16.6788
3	g_X	290.283	1.1845	286.670	1.1399	199.378	9.0406	192.583	2.4662
	g_Y		2.2599		2.2096		5.4273		5.4041
	g_Z		13.2484		13.3596		0.1321		11.2591
4	g_X	359.280	0.8859	352.868	0.9743	217.607	9.3602	211.385	3.0779
	g_Y		3.4859		3.4062		7.4808		3.4811
	g_Z		9.3764		9.5058		0.3755		11.4406
5	g_X	431.146	2.8740	424.226	2.3103	239.960	3.8305	235.811	4.1742
	g_Y		4.8932		5.3646		4.7976		4.7200
	g_Z		11.2780		10.3905		7.9796		7.7895
6	g_X	480.015	0.2629	464.923	0.3403	293.116	0.8327	285.788	0.8929
	g_Y		1.8441		2.3637		2.8442		3.0628
	g_Z		13.8972		14.0858		12.3145		12.2550
7	g_X	540.820	0.8505	511.156	1.1348	316.491	2.0970	308.481	2.1935
	g_Y		0.9930		1.3056		2.5583		3.7919
	g_Z		17.8734		17.7406		8.0156		7.2177
8	g_X	593.619	0.0836	561.349	0.1227	347.899	11.0588	338.596	10.9659
	g_Y		0.2718		0.4484		8.2791		8.3134
	g_Z		19.2422		18.9589		2.4657		2.6402

Table S22. Angles between the main magnetic axes of the lowest Kramers doublet obtained in different computational approximations (degrees)

	AA	AB	BA	BB
AA	0.000	0.202	5.312	4.860
AB	0.202	0.000	5.494	5.041
BA	5.312	5.494	0.000	0.462
BB	4.860	5.041	0.462	0.000

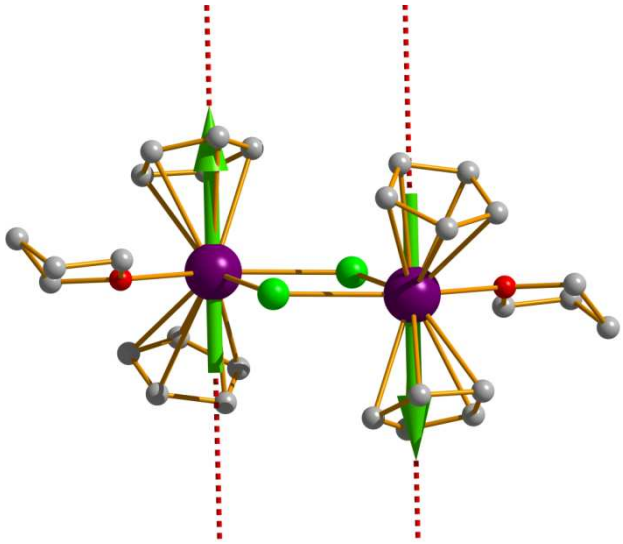

Figure S21. Orientation of the main anisotropy axes of the ground Kramers doublet of **4**. Green arrows show the antiferromagnetic coupling of the local magnetic moments of the Dy ions in the ground state. The main anisotropy axis of the ground state is almost perpendicular to the Dy_2Cl_2 plane (see Table S23).

Table S23. Angles between the main magnetic axes of the lowest Kramers doublet obtained in different computational approximations and the Dy_2Cl_2 plane [°].

	AA	AB	BA	BB
angle	85.918	86.122	80.806	81.268

Table S24. Exchange interactions between Dy ions in the complex **4**.

Lines parameters (cm^{-1}):

	AA	AB	BA	BB
J_{exch}	-0.01504	-0.01462	0.00131	0.00342
$J_{dipolar}$	-0.08264	-0.08267	-0.07933	-0.07963
$J_{total}=J_{exch}+J_{dipolar}$	-0.09768	-0.09729	-0.07802	-0.07621

Ising parameters (cm^{-1}):

	AA	AB	BA	BB
J_{exch}	-0.37600	-0.36550	0.03275	0.08550
$J_{dipolar}$	-2.06600	-2.06675	-1.98325	-1.99075
$J_{total}=J_{exch}+J_{dipolar}$	-2.44200	-2.43225	-1.95050	-1.90525

Table S25. Energies and corresponding tunnelling gaps of the lowest five exchange doublet states of **4**.

AA		AB		BA		BB	
energy	Δ_t	energy	Δ_t	energy	Δ_t	energy	Δ_t
0.000000000 0.000000000	0.000E+00	0.000000000 0.000000003	3.000E-09	0.000000000 0.000003809	3.809E-06	0.000000000 0.000006724	6.724E-06
1.144516713 1.144516735	2.200E-08	1.138163910 1.138164624	7.140E-07	0.856247453 0.856253840	6.387E-06	0.831590697 0.831601244	1.055E-05
161.833818440 161.833819021	5.810E-07	159.078690316 159.078690615	2.990E-07	97.574960436 97.574963186	2.750E-06	95.775407560 95.775412459	4.899E-06
162.015213255 162.015213320	6.500E-08	159.261972732 159.261972789	5.700E-08	97.784984811 97.785015989	3.118E-05	95.997731367 95.997785509	5.414E-05
162.896258908 162.896259848	9.400E-07	160.134086203 160.134087259	1.056E-06	98.386427995 98.386471070	4.308E-05	96.558291870 96.558367035	7.516E-05

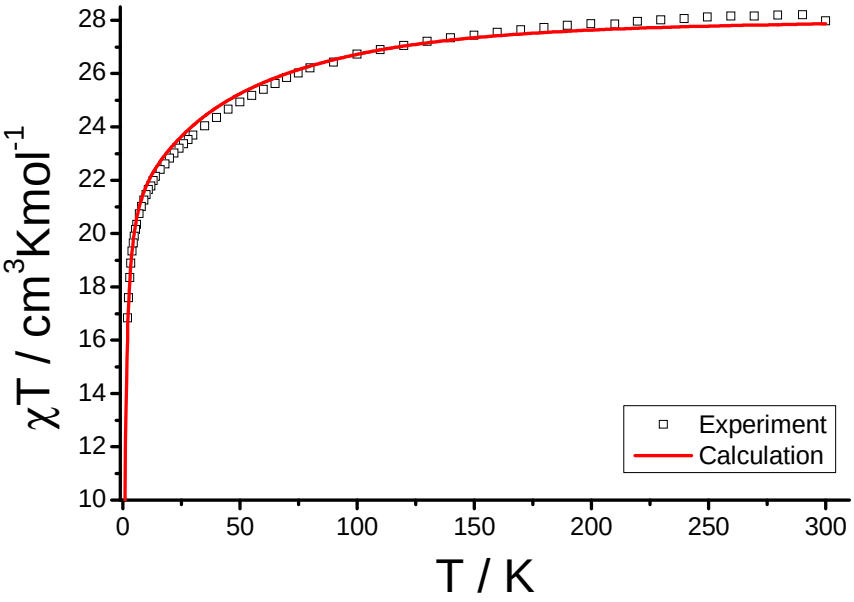

Figure S22. A comparison between measured and calculated magnetic susceptibility of **4** (computational approximation BB).

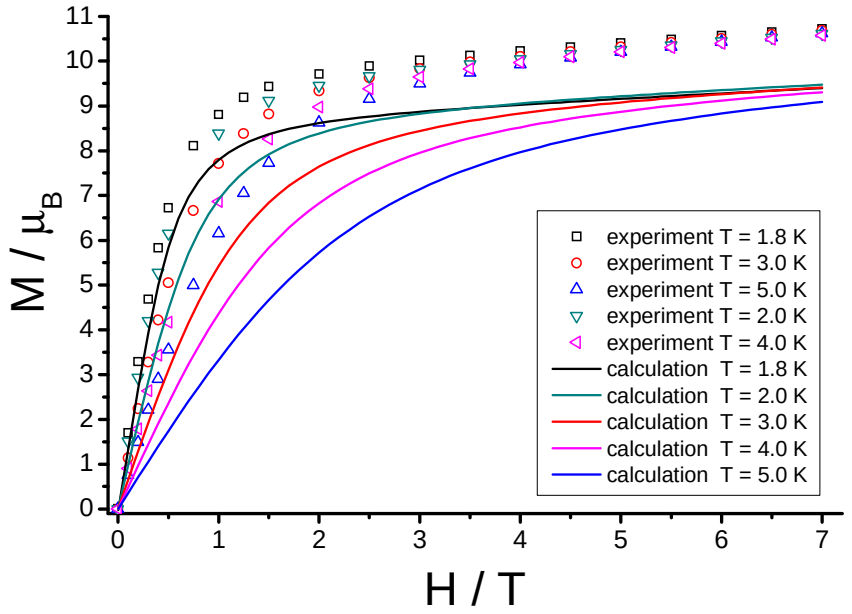

Figure S23. Measured and calculated molar magnetization of **4** at low temperature (computational approximation BB).

Local electronic and magnetic properties of the $[Cp_2Dy(\mu\text{-Bta})]_2$ (5).

Table S26. Energies of the lowest Kramers doublets (cm^{-1}) on individual Dy ions in **5**.

Kramers doublets (cm^{-1})			
AA	AB	BA	BB
0.000	0.000	0.000	0.000
156.787	154.838	103.453	103.949
286.117	283.001	171.433	171.728
328.107	322.147	207.302	210.283
355.178	344.782	227.282	226.287
380.156	371.282	246.530	248.792
430.299	421.406	296.143	295.570
537.679	523.073	395.202	389.575
3617.453	3614.105	3597.226	3595.429
3736.311	3729.905	3669.038	3666.461
3799.132	3789.703	3698.320	3695.629
3856.906	3846.516	3738.403	3735.886
3911.242	3901.116	3768.975	3768.123
3945.928	3933.490	3817.939	3813.477
3983.090	3967.130	3840.838	3834.661
6181.302	6175.449	6128.144	6125.860
6259.936	6250.634	6182.571	6178.272
6321.396	6310.094	6231.093	6226.065
6393.991	6381.639	6264.315	6260.832
6452.667	6440.032	6327.896	6322.725
6484.990	6468.141	6345.569	6338.358
8159.540	8151.391	8090.348	8086.865
8204.030	8192.764	8112.428	8107.462
8310.859	8297.583	8203.901	8198.039
8381.637	8368.288	8270.529	8264.138
8428.636	8411.327	8294.673	8286.489
9685.889	9676.239	9620.245	9615.586
9768.114	9755.253	9665.790	9659.986
9850.842	9836.894	9721.044	9714.652
9981.830	9964.249	9868.276	9858.955
…	…	…	…

Table S27. Energies (cm^{-1}) and g tensors of the lowest Kramers doublets (KD) on individual Dy ions in **5**.

KD		AA		AB		BA		BB	
		E (cm^{-1})	*g*	E (cm^{-1})	*g*	E (cm^{-1})	*g*	E (cm^{-1})	*g*
1	g_X	0.000	0.0128	0.000	0.0148	0.000	0.0038	0.000	0.0073
	g_Y		0.0347		0.0405		0.0761		0.0884
	g_Z		19.5065		19.5777		19.0472		19.0530
2	g_X	156.787	0.0011	154.838	0.0201	103.453	0.1313	103.949	0.1668
	g_Y		0.0437		0.0708		0.4598		0.5096
	g_Z		16.8989		16.9308		16.3546		16.2998
3	g_X	286.117	2.1375	283.001	2.5531	171.433	0.4593	171.728	0.4305
	g_Y		3.3995		3.8282		1.0073		0.8721
	g_Z		13.2048		12.8940		17.7649		17.7264
4	g_X	328.107	3.6333	322.147	3.2064	207.302	9.7942	210.283	9.9004
	g_Y		4.3517		3.9459		8.5526		8.0373
	g_Z		10.1635		10.9991		2.7509		3.0418
5	g_X	355.178	0.0411	344.782	0.1032	227.282	0.4708	226.287	1.0896
	g_Y		2.1565		1.9827		1.9148		2.0250
	g_Z		12.9548		13.6686		13.2599		13.2705
6	g_X	380.156	1.6707	371.282	1.8081	246.530	2.6683	248.792	3.2617
	g_Y		3.3537		2.9695		4.5624		4.4623
	g_Z		8.2917		9.2784		6.7181		6.5340
7	g_X	430.299	1.6805	421.406	1.8620	296.143	2.6553	295.570	2.6652
	g_Y		5.4708		5.1086		5.6856		5.4363
	g_Z		12.1073		12.3309		10.9842		11.1710
8	g_X	537.679	0.3154	523.073	0.3730	395.202	0.3517	389.575	0.3743
	g_Y		0.6361		0.7567		0.5007		0.5409
	g_Z		18.8516		18.8199		18.6041		18.5745

Table S28. Angles between the main magnetic axes of the lowest Kramers doublet obtained in different computational approximations [°].

	AA	AB	BA	BB
AA	0.000	0.053	3.626	3.407
AB	0.053	0.000	3.677	3.458
BA	3.626	3.677	0.000	0.225
BB	3.407	3.458	0.225	0.000

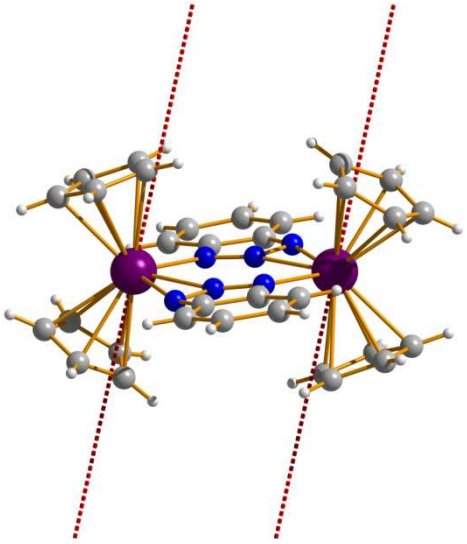

Figure S24. Orientation of the main anisotropy axes of the ground Kramers doublet of **5**.